HERA: Illuminating Our Early Universe

For the Mid-Scale Science Projects category of the Mid-Scale Innovations Program

The Hydrogen Epoch of Reionization Arrays (HERA) roadmap is a staged program that uses the unique properties of the 21 cm line from neutral hydrogren to probe the Epoch of Reionization (EoR) and the preceding Dark Ages. These epochs correspond to when the first stars and black holes heat and reionize the Universe following cosmic recombination, roughly 0.3 Gyr to 1 Gyr after the Big Bang. Direct observation of the evolution of the large scale structure of reionization via the HI 21 cm line will have a profound impact on our understanding of the birth of the first galaxies and black holes, their influence on the intergalactic medium (IGM), and cosmology.

HERA was ranked the "top priority in the Radio, Millimeter, and Sub-millimeter category of recommended new facilities for mid-scale funding" as part of the *New Worlds, New Horizons of Astronomy and Astrophysics* decadal survey (Comm. for a Decadal Survey of A&A; NRC 2010; hereafter NWNH). The HERA roadmap envisioned a series of radio interferometers constructed throughout the decade, starting with the current Donald C. Backer Precision Array to Probe the Epoch of Reionization (PAPER) and the Murchison Widefield Array (MWA) instruments aimed at characterizing foregrounds and laying the groundwork for detecting the EoR power spectrum. A second-generation HERA instrument would measure the EoR power spectrum in detail and reveal how early structure in the Universe formed, and a third-generation instrument would map EoR.

Using the advances spearheaded by PAPER and the MWA, we propose to build the next generation of HERA in stages of 127, 331, and 568 elements, observing in the 50–225MHz band. Each stage of HERA is scoped to deliver new science capabilities that advance our understanding of reionization in a timely manner:

- HERA 127 will measure the rise and fall of the EoR power spectrum, constraining the timing and duration of reionization.
- HERA 331 will measure the shape of the power spectrum over a significant range in wavenumber, determining the features and distribution of the first galaxies that dominate cosmic reionization.
- HERA 568 will extend precision power-spectrum observations into the Dark Ages and start direct imaging of the IGM during reionization.

Taken together, this program not only fulfills the NWNH goal of detailed power spectrum characterization as a second-generation EoR experiment, but is also capable of imaging the EoR—a task previously considered possible only for third-generation instruments.

1. Scientific Justification

The last unexplored phase in the evolution of luminous structures in the Universe begins with the birth of the first stars and culminates with the full ionization of the IGM ∼500 Myrs later. During the Dark Ages ($z \geq 15$) and the Epoch of Reionization ($z \sim 15$–6), a wealth of astrophysical and cosmological phenomena are at work. The precise properties of the IGM depend on the nature and distribution of the first luminous sources (eg. typical masses, UV escape fractions, biased structure formation), the efficiency and abundance of heating sources (eg. X-ray binaries, shocks, or even dark matter annihilations), the formation of the first supermassive black holes, and the relative velocity of baryonic matter and dark-matter halos, among other effects. Exploring the Dark Ages and EoR, and the evolution of the IGM during these epochs, was one of the top three "priority science objectives chosen by the [NWNH] survey committee for the decade 2012-2021."

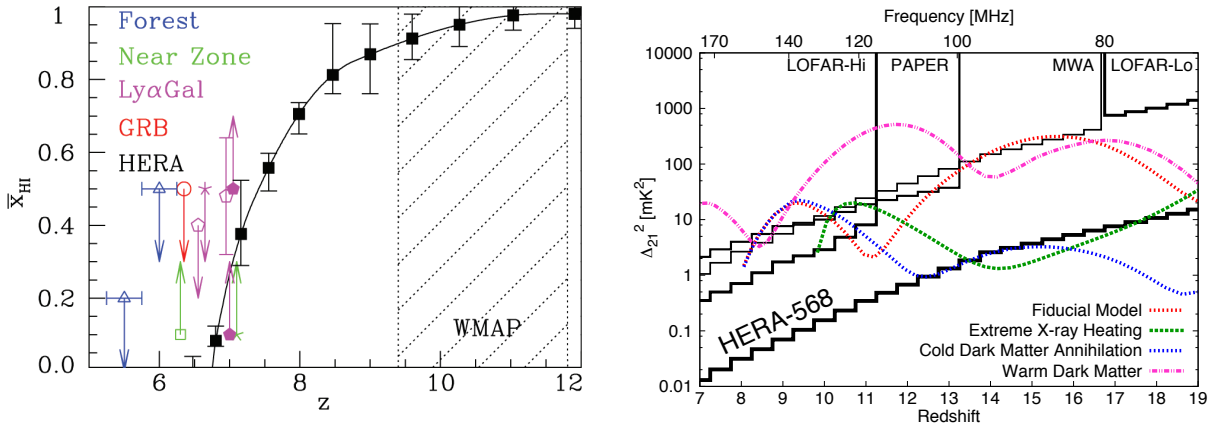

Fig. 1.— Left: Adapted from Robertson et al. (2013), this figure shows existing constraints on $x_{\rm HI}$ during reionization (colored symbols), along with a reionization history consistent with these measurements (black line). The constraints HERA would provide are indicated with black markers (with the constraint that $x_{\rm HI}$ steadily decreases over this redshift range). At redshifts 8–12 21 cm emission may be the only precision probe of the neutral fraction. Right: HERAs substantial sensitivity at low frequencies opens a window to pre-reionization physics. Shown here are power spectrum amplitudes (at $k = 0.15h$ Mpc^{-1}) as a function of redshift for various IGM heating models, along with predicted sensitivities.

So far, a number of indirect probes have been used to understand cosmic reionization. These include observations of Gunn-Peterson absorption by the IGM toward distant quasars (Fan et al. 2006), kinetic Sunyaev-Zel'dovich anisotropies in the CMB temperature (Zahn et al. 2012), CMB polarization (Page et al. 2007; Planck Collaboration et al. 2013), and the demographics of Lyα emitting galaxies (Treu et al. 2013), as summarized in Figure 1a. Unfortunately, these ground-breaking results have limited reach: the Gunn-Peterson effect and related phenomena saturate at low neutral fractions, and the CMB provides only an integral measure of the EoR looking back to recombination. Moreover, many of these indirect observations are in tension with one another, underscoring both the difficulty in their interpretation and the complexity of the reionization process.

As a high sensitivity instrument with broad frequency coverage, HERA will be perhaps the most powerful probe of the evolution of the IGM during cosmic reionization, and into the preceding Dark Ages. The black line in Figure 1a indicates a model from Robertson et al. (2013) that is consistent with current constraints on reionization. The black symbols and error bars show how HERA would measure the evolution of the neutral fraction throughout the EoR, definitively answering how reionization occurred. The wide range of heating and ionization models HERA can constrain during the EoR and into the Dark Ages is captured in Figure 1b. As emphasized in NWNH: "The panel concluded that to explore the discovery area of the epoch of reionization, it is most important to develop new capabilities to observe redshifted 21 cm HI emission, building on the legacy of current projects and increasing sensitivity and spatial resolution to characterize the topology of the gas at reionization."

In the past decade, considerable effort has gone into modeling the complex astrophysics of reionization (e.g. Santos et al. 2010; Mesinger et al. 2011; Wyithe and Loeb 2004). However, basic constraints on theoretical models are still rudimentary and the most fundamental questions concerning the process of reionization remain open. When did reionization occur, and over what

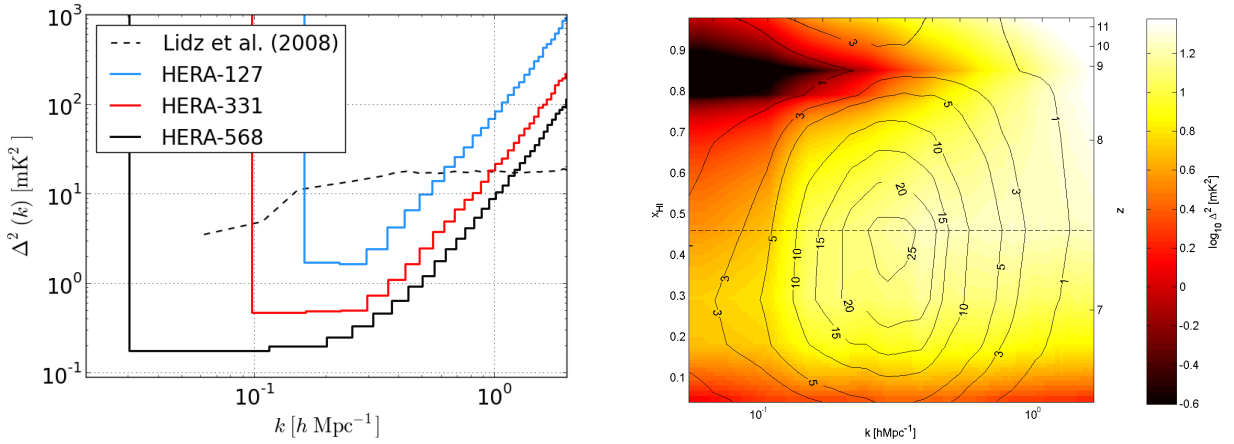

Fig. 2.— Left: Power-spectrum sensitivities for three stages of HERA (solid) relative to a fiducial ionization model (dashed line at $x_{\rm HI} = 0.47$ in both panels). In addition to a staged array size, sensitivity curves reflect a staged improvement in analysis software that expands the range of modes that are not corrupted by systematics. Right: The color surface shows the rise and fall of the 21 cm power spectrum from Lidz et al. 2008 as a function of neutral fraction $x_{\rm HI}$ (and hence redshift). The spectrum initially follows the dark matter fluctuations at the upper edge of the plot, falls as the densest regions reionize at $x_{\rm HI} = 0.8$, rises and flattens as galaxies ionize large bubbles in the IGM ($0.6 < x_{\rm HI} < 0.2$), and finally falls again as reionization completes at the bottom of the plot. Contours indicate the predicted signal-to-noise ratio of HERA 568 observations throughout reionization.

timescale? What objects dominated the radiation field? How were the objects distributed? Did the first generation of stars enhance or suppress the formation of subsequent stars in the original halo and smaller nearby halos? Without measurements from a HERA-like experiment, further progress on understanding first galaxy formation and cosmic reionization will remain problematic.

2. Foregrounds & Lessons Learned from PAPER and MWA

The key challenge of 21 cm cosmology is isolating the faint EoR signal from astrophysical foregrounds that are ∼5 orders of magnitude brighter. These foregrounds are shown in recent MWA image in the left-hand panel of Figure 3. A major breakthrough in 21 cm cosmology—what enables us to propose HERA now—is the discovery of the EoR Window.

21 cm cosmology observations and foreground isolation are best understood in the three dimensional wavenumber space **k**. Because the HI emission is a narrow spectral line, the observed frequency of the emission can be mapped to redshift or line-of-sight distance to provide an observed volume $\{x, y, z\}$ in co-moving Mpc. This observed volume is Fourier transformed into a three dimensional wavenumber cube $\{k_x, k_y, k_z\}$. For graphical simplicity, the angular wavenumbers are typically averaged ($\{k_x, k_y\} \rightarrow k_\perp$) to produce line-of-sight wavenumber $k_\parallel$ vs. angular $k_\perp$. The expected statistical isotropy of the signal allows measurements within the 3D wavenumber space to be squared and averaged in shells to produce the spherical power spectrum presented in Figure 2.

A significant recent advance in 21 cm cosmology has been understanding how smooth-spectrum foreground emission interacts with the instrument to produce the EoR Window. Through a concerted theoretical and observational campaign (Morales et al. 2012; Parsons et al. 2012; Vedantham et al. 2012; Datta et al. 2010; Hazelton et al. 2013; Pober et al. 2013; Parsons et al. 2013; Dillon

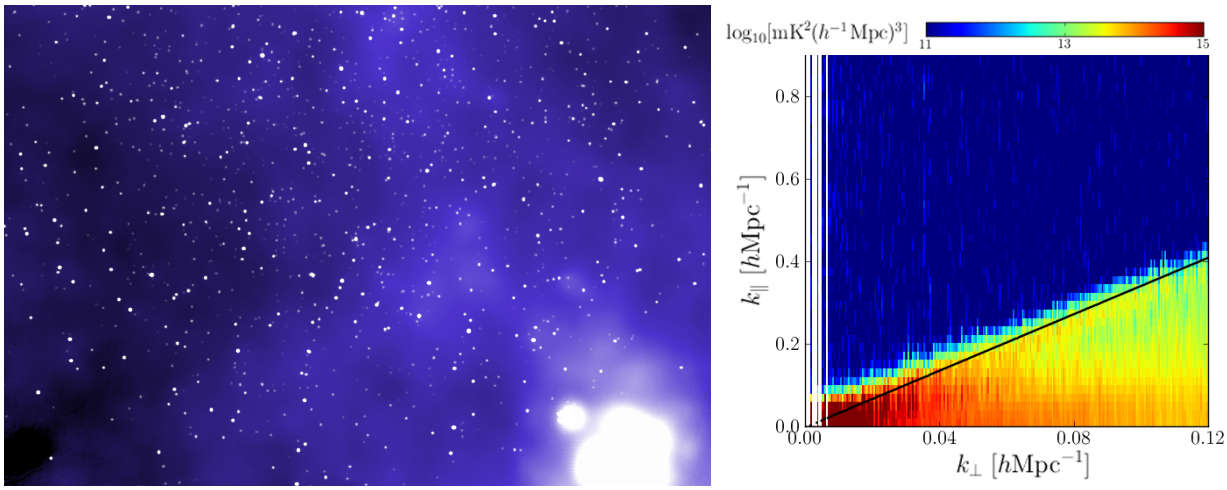

Fig. 3.— Left: Foregrounds imaged on the MWA using FHD software developed by Morales' group (Sullivan et al. 2012). This image spans ∼30° and includes both point-source and diffuse emission (with the Vela and Puppis SNRs visible in the bottom-right), illustrating the power of imaging methods for reducing polarization leakage and foreground systematics. Right: Foreground contamination in line-of-sight $k_\parallel$ vs. angular $k_\perp$ as observed using PAPER (Pober et al. 2013), with the analytic prediction of the horizon limit to foreground emission (solid black). Bright foreground emission is confined to a wedge (lower right) as predicted by (Morales et al. 2012; Parsons et al. 2012; Vedantham et al. 2012; Datta et al. 2010), and falls by orders-of-magnitude in the EoR Window (blue region), where measurements are currently thermal noise limited. This insight has lead to the first meaningful constraints on EoR via 21 cm emission in Parsons et al. (2013).

et al. 2013) we now understand that the foreground contamination is confined to a 'wedge' in $k_\parallel$ vs. $k_\perp$, as demonstrated by the PAPER observations in the righthand panel of of Figure 3. This wedge is the result of the smooth spectrum foregrounds (low $k_\parallel$) interacting with the inherent chromaticity of an interferometer. Deep imaging similarly suppresses the contributions from polarized foregrounds (Bernardi et al. 2013; Moore et al. 2013). This leaves the region above the wedge isolated from the foreground emission—a window through which we can observe the EoR.

Observations with PAPER and the MWA have now confirmed the presence of the EoR Window (Pober et al. 2013; Dillon et al. 2013), including suppression by more than 4 orders-of-magnitude (8 in mK^2) to the thermal noise floor of current PAPER observations (Parsons et al. 2013). This is a major advance; we can suppress foregrounds and we understand the instrumental and analysis characteristics needed to perform the EoR measurement. The MWA and PAPER teams have been at the forefront of developing the EoR Window, writing all of the papers in the literature and developing the delay-spectrum and full power-spectrum (imaging) analyses to exploit this insight.

3. HERA

HERA will be built in stages at the Karoo Radio Observatory reserve in South Africa near the current PAPER deployment, up to a final size of 568 antenna elements. HERA incorporates numerous lessons learned from first-generation 21 cm EoR experiments. It features a 14-m zenith-pointing dish optimized for sensitivity and foreground suppression, a dense hexagonal core to facilitate redundant baseline calibration and delay-spectrum analysis (see Figure 4), and a distribution of outrigger antennas to provide complete uv coverage to ∼700 m for foreground imaging and mitigation. HERA draws on the technical heritage of the MWA, PAPER, EDGES and MITEoR. Specific

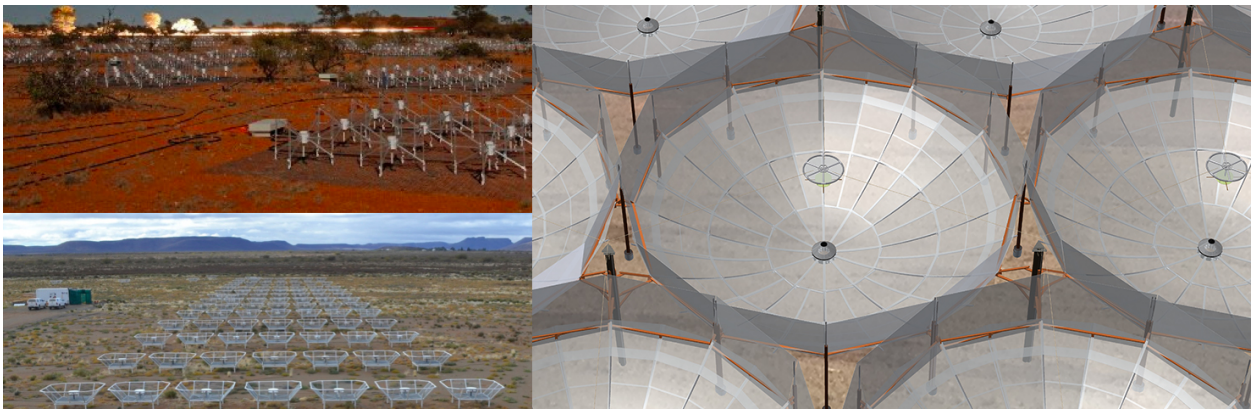

Fig. 4.— The MWA (top left) and PAPER (bottom right) arrays, each currently deployed with 128 elements. The 14-m HERA element (right) dramatically improves sensitivity while delivering the spectral smoothness and stability of response that are required for managing foregrounds. The core of HERA 568 consists of a redundant hexagonal array with outrigger antennas (not shown) for imaging and foreground mitigation.

examples include the antenna feed and correlator of PAPER, receiver node and field digitization from the MWA, absolute radiometric calibration from EDGES, redundant baseline calibration from MITEoR (Zheng et al. 2013), the delay-spectrum analysis from PAPER, and the precision imaging and foreground removal software from the MWA.

The HERA antenna is an example of this technical heritage. The spectral smoothness and the stability of the antenna response determine the precision to which astrophysical foreground emission can be separated from the cosmological 21 cm emission. HERA uses the PAPER dipole feed—modified slightly for wider bandwidth—suspended over a 14-m parabolic dish (Figure 4). The short ($\sim$5 m) focal height of the dishes is central to limiting the path length of reflections, whose time-delay gives rise to chromatic antenna sensitivity. The zenith pointing enhances the stability of the antenna response (as found for PAPER), short cables to in-field digitizers limit the length of cable reflections (MWA), and absolute calibration (EDGES) provide an extremely stable and smooth spectral response. Similarly, the antenna layout features outriggers and a symmetric configuration (MWA), combined with a core of equally spaced elements that improves sensitivity and enables redundancy-based calibration (PAPER, MITEoR). Together these advances enable HERA achieve the science goals envisioned in the decadal survey at a fraction of the cost.

HERA follows a staged deployment in both physical construction and scientific processing. In each deployment stage, improvements are incorporated into the system and new science capabilities are unlocked. This approach has the advantage of both providing early access to science and reducing the project risk by testing systems early and changing them incrementally. As shown in Figure 2, each stage of HERA brings an associated improvement in sensitivity that allows key aspects of 21 cm reionization science to be addressed. The timeline of HERA development, along with the associated science products, is outlined below.

Year 1–Infrastructure and First 37 Antennas (FY 2015).

- Install infrastructure $\sim$10 km from the current PAPER site at the Karoo Radio Observatory in South Africa. Includes ground leveling, power and basic network connectivity.
- Move existing PAPER-128 antennas, correlator, and EMC container to new site.
- Install first 37 HERA antennas and instrument with existing PAPER feeds and electronics.

- Begin development of improved HERA baluns, receivers, feeds, and nodes using the PAPER and MWA technical heritage (Bradley et al. 2005; Lonsdale et al. 2009; Tingay et al. 2013) and the in-situ antenna calibration system based on EDGES (Rogers and Bowman 2012). Continue development of delay-spectrum (Parsons et al. 2012), Fast Holographic Deconvolution (FHD; Sullivan et al. 2012) and optimal estimator software (Dillon et al. 2013).

Year 2–Hardware Commissioning and Deep Foreground Survey (FY 2016).

- Commissioning observations using a hybrid array of 37 HERA antennas in a close-packed hexagon surrounded by 91 PAPER antennas in an imaging configuration.
- Perform a polarized foreground survey using hybrid-antenna capability of FHD. Determine on-sky beam response of HERA antennas to facilitate future source subtraction efforts.
- Finalize site infrastructure (high-bandwidth optical network, surveying, trenching).
- On-antenna commissioning of new feeds, receivers, nodes, and calibration systems in Green Bank and South Africa.
- Build out to 127 HERA antennas starts.

Year 3–HERA 127 and Detecting the Rise and Fall of Reionization (FY 2017).

- Complete construction of HERA 127. Begin science observations Oct. 2016, again using the PAPER correlator.
- Begin analysis of a dataset capable of constraining the timing and duration of reionization. Analysis focuses on proven techniques based on PAPER delay-spectrum analysis, explorating subtraction of bright and polarized foregrounds.
- Begin deployment of HERA 331. Install node electronics for all 331 elements, and a new 331-element, GPU-based correlator in the Karoo Array Processing Building (KAPB).
- Install new data storage infrastructure in the KAPB. Upgrade the UPenn analysis cluster.

Year 4–HERA 331 and Measuring the Evolution of the First Galaxies (FY 2018).

- Finish construction of HERA 331. Begin science observations Oct. 2017.
- Complete science observations with HERA 331 Apr. 2018. Begin analysis of data to characterize the evolution of the power spectrum and determining properties of the first galaxies.
- Continue analysis software development, emphasizing imaging-based subtraction techniques for expanding the EoR window.
- Begin build out to 568 antennas begins, including outrigger antennas to facilitate imaging and better foreground removal.
- Complete pipelines for EoR processing of HERA 568.

Year 5–HERA 568, Imaging Reionization and Exploring the Dark Ages (FY 2019).

- Finish construction of HERA 568. Begin science observations Oct. 2018.
- Analysis push to enable imaging of the largest structures and extracting the full sensitivity of the instrument, including partially coherent baselines.

The staged buildout of HERA enables cutting edge science at each stage while mitigating risk by allowing the team to learn from experience along the way. HERA 127 will measure the rise and fall of the EoR power spectrum; HERA 331 will characterize the shape of the power spectrum and constrain the development of the first galaxies; and HERA 568 will start to image reionization while pushing power spectrum measurements into the Dark Ages.

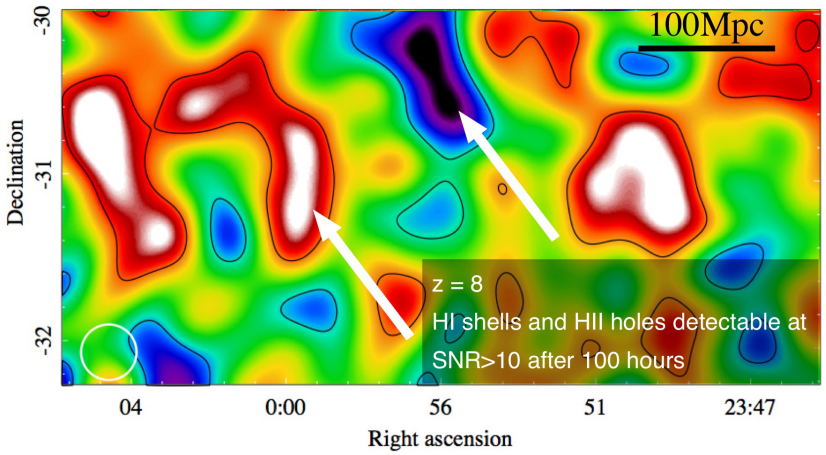

Fig. 5.— A simulated imaging reconstruction of HI emission at $z = 8$ from 100 hours of HERA 568 observations with 1 MHz of bandwidth. The resulting EoR map has a resolution of $20'$(∼50 cMpc); black contours enclose regions detected at 10σ. With a surface brightness sensitivity of 60 μJy after filtering chromatic foregrounds, HERA has the sensitivity to directly image regions of neutral and ionized hydrogen.

4. Broader Impacts

An important part of the HERA program is training new instrumentalists. The project plan involves graduate students in all stages of HERA development and observation. We will also fund an undergraduate specialist position at UC Berkeley's RAL, offered annually, with the goal of mentoring the individual in the skills required to pursue graduate research in instrumentation.

A second important activity of the HERA program is the diversity efforts that naturally afford themselves working in Africa. PAPER has an admirable history of enlisting interns from South African Universities as part of major engineering deployments, with the work applied as practical training within their academic program. For HERA, we are establishing formal collaborations with South African faculty, to engage doctoral students from these institutions in HERA, including working visits between students in both directions. We will recruit talented South African undergraduate and masters students for 3-month internships at the HERA partner institutions. Each year, one institution will host the SA student team, providing an REU-like experience focused on helping commission and operate HERA. This experience will familiarize the students with US graduate education, and give them the research experience and professional contacts needed to successfully apply for graduate education the USA, should they choose to do so.

Public Data Products. On the HERA timescale a number of new observations will come on line that would benefit from cross-comparison with the power spectra and images produced by HERA. These include providing the reionization environment for JWST and ALMA galaxy and cluster observations; cross-correlation with WFIRST near-IR surveys; and cross-correlation with CMB polarization observations. The HERA measurements will be released to the community after an 18 month proprietary period and hosted at MIT. These data products will include foreground subtracted cubes for cross-correlation, deep images of reionization from HERA 568, compressed visibilities for re-analysis, snapshot continuum images for transient observations, and wide-field maps from the survey made in the first two years.

5. Project Management Plan

This project balances the light-weight management structure of current PAPER/MWA activities and the more formal structure required for larger-scale projects. Construction management is centered at UC Berkeley's Radio Astronomy Laboratory (RAL), headed by Parsons as the Project Director and DeBoer as Project Manager. They are assisted by Bob Goeke at MIT as a part-time Project Engineer with emphasis on interfacing with the US-based antenna contractor. A Site Manager splits time between South Africa and Berkeley and manages the construction activities by local South African contractors. A SKA-SA Liaison coordinates HERA, Meerkat, and SKA site activities (supported by SKA-SA). Governance is provided by an Executive Board comprising this proposal's senior investigators that operates using super-majority policies.

The scientific capability of HERA and the data analysis and publication are overseen by the Science Panel, and chaired by the Project Scientist, Bowman. These positions rotate as needed expertise changes, and are appointed by the Executive Board. As with the MWA and PAPER, observing proceeds remotely with limit site support and maintenance, headed by the Site Manager.

The estimated inherent contingency is $\sim$15%, anticipating that additional project risk and contingency are handled by reducing build-out with associated de-scoping of science capabilities. A baseline design using existing hardware establishes a low-risk path to core functionality and science. Improved functionality results from successful development activities or is otherwise de-scoped.

6. Why Now? Why Us?

This HERA proposal follows the vision for 21 cm observations laid out in NWNH. PAPER and the MWA have already succeeded in the primary task envisioned in NWNH—characterizing the astrophysical foregrounds and developing the hardware and analysis advances needed to suppress the contamination. The discovery and characterization of the EoR Window and the development of precision foreground mitigation techniques have shown that foregrounds can be suppressed to the current level thermal noise (§2; Parsons et al. 2013). While the MWA and PAPER are pushing hard to detect the EoR power spectrum, a marginal detection is the best these instruments can achieve. HERA will both ensure a high significance detection of the HI 21 cm signal, as well as provide powerful constraints on the rise and fall of reionization, how early stars and structure formed, and physical processes at the end of the cosmic dark ages (Figures 1 & 2).

As envisioned in NWNH, the US EoR projects (PAPER, MWA, EDGES, MITEoR) have pooled their expertise to develop the second generation HERA observatory. This has created a collaborative team with a deep well of scientific experience—the majority of papers on EoR observations are authored by members of the HERA team. By leveraging this expertise, the HERA design is significantly less expensive than envisioned in NWNH, and has greater scientific reach.

The last few years have been productive—we understand foreground systematics and are pushing current instruments to their thermal limits. We are now ready to build the HERA instrument envisioned in NWNH and realize the scientific promise of 21 cm cosmology. Studying the formation of the first luminous structures after the Big Bang and how they reionize the Universe is a primary driver for major astronomical facilities over the next decade (ref: NWNH). Such studies include direct observation of stars, gas, dust, and AGN in the first galaxies using the JWST, TMT, ALMA, CCAT, and the JVLA. HERA is a unique and necessary element in this panchromatic arsenal, providing the large scale context in which the complex process of first galaxy formation plays out.

References

Barkana, R. and A. Loeb, 2005: A Method for Separating the Physics from the Astrophysics of High-Redshift 21 Centimeter Fluctuations. *ApJ*, **624**, L65–L68, arXiv:astro-ph/0409572.

Bernardi, G., L. J. Greenhill, D. A. Mitchell, S. M. Ord, and 49 co-authors, 2013: A 189 MHz, 2400 deg^2 Polarization Survey with the Murchison Widefield Array 32-element Prototype. *ApJ*, **771**, 105, 1305.6047.

Bradley, R., D. Backer, A. Parsons, C. Parashare, and N. E. Gugliucci, 2005: PAPER: A Precision Array to Probe the Epoch of Reionization. In *Bulletin of the American Astronomical Society*, vol. 37, pp. 1216–+.

Comm. for a Decadal Survey of A&A; NRC, 2010: *New Worlds, New Horizons in Astronomy and Astrophysics*. Natl. Academies Press.

Datta, A., J. D. Bowman, and C. L. Carilli, 2010: Bright Source Subtraction Requirements for Redshifted 21 cm Measurements. *ApJ*, **724**, 526–538, 1005.4071.

Dillon, J. S., A. Liu, M. Tegmark, G. Bernardi, and 55 co-authors, 2013: Overcoming Real-World Obstacles in 21 cm Power Spectrum Estimation: A Demonstration and Results from Early Murchison Widefield Array Data. *ArXiv*, 1304.4229.

Fan, X., C. L. Carilli, and B. Keating, 2006: Observational Constraints on Cosmic Reionization. *ARA&A*, **44**, 415–462, arXiv:astro-ph/0602375.

Furlanetto, S. R., S. P. Oh, and F. H. Briggs, 2006: Cosmology at low frequencies: The 21 cm transition and the high-redshift Universe. *Phys. Rep.*, **433**, 181–301, arXiv:astro-ph/0608032.

Hazelton, B. J., M. F. Morales, and I. S. Sullivan, 2013: The Fundamental Multi-Baseline Mode-Mixing Foreground in 21 cm EoR Observations. *ArXiv*, 1301.3126.

Lidz, A., O. Zahn, M. McQuinn, M. Zaldarriaga, and L. Hernquist, 2008: Detecting the Rise and Fall of 21 cm Fluctuations with the Murchison Widefield Array. *ApJ*, **680**, 962–974, arXiv:0711.4373.

Loeb, A. and M. Zaldarriaga, 2004: Measuring the Small-Scale Power Spectrum of Cosmic Density Fluctuations through 21cm Tomography Prior to the Epoch of Structure Formation. *Physical Review Letters*, **92(21)**, 211301–+, arXiv:astro-ph/0312134.

Lonsdale, C. J., R. J. Cappallo, M. F. Morales, F. H. Briggs, and 43 co-authors, 2009: The Murchison Widefield Array: Design Overview. *IEEE Proceedings*, **97**, 1497–1506, 0903.1828.

Mesinger, A., S. Furlanetto, and R. Cen, 2011: 21CMFAST: a fast, seminumerical simulation of the high-redshift 21-cm signal. *MNRAS*, **411**, 955–972, 1003.3878.

Moore, D. F., J. E. Aguirre, A. R. Parsons, D. C. Jacobs, and J. C. Pober, 2013: The Effects of Polarized Foregrounds on 21 cm Epoch of Reionization Power Spectrum Measurements. *ApJ*, **769**, 154, 1302.0876.

Morales, M. F., B. Hazelton, I. Sullivan, and A. Beardsley, 2012: Four Fundamental Foreground Power Spectrum Shapes for 21 cm Cosmology Observations. *ApJ*, **752**, 137, 1202.3830.

Morales, M. F. and J. S. B. Wyithe, 2010: Reionization and Cosmology with 21-cm Fluctuations. *ARA&A*, **48**, 127–171, 0910.3010.

Page, L., G. Hinshaw, E. Komatsu, M. R. Nolta, D. N. Spergel, C. L. Bennett, C. Barnes, R. Bean, O. Doré, J. Dunkley, M. Halpern, R. S. Hill, N. Jarosik, A. Kogut, M. Limon, S. S. Meyer, N. Odegard, H. V. Peiris, G. S. Tucker, L. Verde, J. L. Weiland, E. Wollack, and E. L. Wright, 2007: Three-Year Wilkinson Microwave Anisotropy Probe (WMAP) Observations: Polarization

Analysis. *ApJS*, **170**, 335–376, arXiv:astro-ph/0603450.

Parsons, A. R., A. Liu, J. E. Aguirre, Z. S. Ali, R. F. Bradley, C. L. Carilli, D. R. DeBoer, M. R. Dexter, N. E. Gugliucci, D. C. Jacobs, P. Klima, D. H. E. MacMahon, J. R. Manley, D. F. Moore, J. C. Pober, I. I. Stefan, and W. P. Walbrugh, 2013: New Limits on 21cm EoR From PAPER-32 Consistent with an X-Ray Heated IGM at z=7.7. *ArXiv*, 1304.4991.

Parsons, A. R., J. C. Pober, J. E. Aguirre, C. L. Carilli, D. C. Jacobs, and D. F. Moore, 2012: A Per-baseline, Delay-spectrum Technique for Accessing the 21 cm Cosmic Reionization Signature. *ApJ*, **756**, 165, 1204.4749.

Planck Collaboration, P. A. R. Ade, N. Aghanim, C. Armitage-Caplan, M. Arnaud, M. Ashdown, F. Atrio-Barandela, J. Aumont, C. Baccigalupi, A. J. Banday, and et al., 2013: Planck 2013 results. XVI. Cosmological parameters. *ArXiv*, 1303.5076.

Pober, J. C., A. R. Parsons, J. E. Aguirre, Z. Ali, R. F. Bradley, C. L. Carilli, D. DeBoer, M. Dexter, N. E. Gugliucci, D. C. Jacobs, P. J. Klima, D. MacMahon, J. Manley, D. F. Moore, I. I. Stefan, and W. P. Walbrugh, 2013: Opening the 21 cm Epoch of Reionization Window: Measurements of Foreground Isolation with PAPER. *ApJ*, **768**, L36, 1301.7099.

Robertson, B. E., S. R. Furlanetto, E. Schneider, S. Charlot, R. S. Ellis, D. P. Stark, R. J. McLure, J. S. Dunlop, A. Koekemoer, M. A. Schenker, M. Ouchi, Y. Ono, E. Curtis-Lake, A. B. Rogers, R. A. A. Bowler, and M. Cirasuolo, 2013: New Constraints on Cosmic Reionization from the 2012 Hubble Ultra Deep Field Campaign. *ApJ*, **768**, 71, 1301.1228.

Rogers, A. E. E. and J. D. Bowman, 2012: Absolute calibration of a wideband antenna and spectrometer for accurate sky noise temperature measurements. *Radio Science*, **47**, 0, 1209.1106.

Santos, M. G., L. Ferramacho, M. B. Silva, A. Amblard, and A. Cooray, 2010: Fast large volume simulations of the 21-cm signal from the reionization and pre-reionization epochs. *MNRAS*, **406**, 2421–2432, 0911.2219.

Sullivan, I. S., M. F. Morales, B. J. Hazelton, W. Arcus, D. Barnes, G. Bernardi, F. H. Briggs, J. D. Bowman, and 44 co-authors, 2012: Fast Holographic Deconvolution: A New Technique for Precision Radio Interferometry. *ApJ*, **759**, 17, 1209.1653.

Tingay, S. J., R. Goeke, J. D. Bowman, and 58 co-authors, 2013: The Murchison Widefield Array: The Square Kilometre Array Precursor at Low Radio Frequencies. *PASA*, **30**, 7, 1206.6945.

Treu, T., K. B. Schmidt, M. Trenti, L. D. Bradley, and M. Stiavelli, 2013: The changing Lya optical depth in the range 6<z<9 from MOSFIRE spectroscopy of Y-dropouts. *ArXiv*, 1308.5985.

Vedantham, H., N. Udaya Shankar, and R. Subrahmanyan, 2012: Imaging the Epoch of Reionization: Limitations from Foreground Confusion and Imaging Algorithms. *ApJ*, **745**, 176, 1106.1297.

Wyithe, J. S. B. and A. Loeb, 2004: A characteristic size of ˜10Mpc for the ionized bubbles at the end of cosmic reionization. *Nature*, **432**, 194–196.

Zahn, O., C. L. Reichardt, L. Shaw, A. Lidz, and 47 co-authors, 2012: Cosmic Microwave Background Constraints on the Duration and Timing of Reionization from the South Pole Telescope. *ApJ*, **756**, 65, 1111.6386.

Zheng, H., M. Tegmark, V. Buza, J. S. Dillon, and 32 co-authors, 2013: Mapping our Universe in 3D with MITEoR. *ArXiv*, 1309.2639.